

The Reaction of Hydrogen Bromide with Nitrogen Oxide in Shock Waves

Tetsuo HIGASHIHARA, Ko SAITO,* and Ichiro MURAKAMI

Department of Chemistry, Faculty of Science, Hiroshima University, Higashisenda-machi, Hiroshima 730

(Received March 9, 1978)

The reaction of hydrogen bromide with nitrogen oxide in the temperature range 2000—3300 K and in the pressure range 0.7—3.8 atm has been studied behind reflected shock waves by monitoring the IR emission of HBr. For the early stage of the reaction, the rate equation obtained was $-d[\text{HBr}]/dt = k_{\text{overall}}[\text{HBr}]^{1.0 \pm 0.3}[\text{NO}]^{0.7 \pm 0.2}[\text{Ar}]^{0.0 \pm 0.1}$, where $k_{\text{overall}} = 10^{10.4 \pm 0.2} \exp \{-(23.2 \pm 3.0) \text{ kcal}/RT\} \text{ cm}^2.1 \text{ mol}^{-0.7} \text{ s}^{-1}$. As the initiation step, Reaction 1 was found to be more important than Reaction 2:



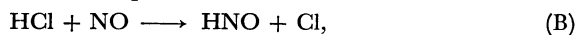
The rate constant of Reaction 1 was determined to be $k_1 = 10^{12.8} \exp(-30 \text{ kcal}/RT) \text{ cm}^3 \text{ mol}^{-1} \text{ s}^{-1}$.

There have been a few previous shock-tube investigations of the reactions of nitrogen oxide with other compounds. Asaba and coworkers^{1,2)} studied the reaction between H_2 and NO, and determined the initiation step and its rate constant to be



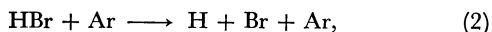
$$k_A = 10^{13.5} \exp(-55.2 \text{ kcal}/RT) \text{ cm}^3 \text{ mol}^{-1} \text{ s}^{-1}.$$

In the previous paper,³⁾ we studied the reaction of HCl with NO. In that work, we found that when nitrogen oxide was added to the HCl-Ar mixture the rate of HCl disappearance was significantly accelerated. On the basis of these experimental results, we discussed the role of NO in the HCl disappearance and determined the initiation step and its rate constant to be



$$k_B = 10^{13.2} \exp(-50.2 \text{ kcal}/RT) \text{ cm}^3 \text{ mol}^{-1} \text{ s}^{-1}.$$

In order to make the role of NO in the disappearance rate of hydrogen halide more clear, we studied the reaction of hydrogen bromide with nitrogen oxide. Since the rate constant of Reaction 2 was determined in the HBr-Ar system by Giedt *et al.*⁴⁾ in the temperature range 2100—4200 K:



the influence of NO on the rate of HBr disappearance could be investigated by adding NO to the HBr-Ar system.

Experimental

The shock tube was 5 cm in internal diameter, and had a 3.8 cm long test section. The side of the tube was fitted with a CaF_2 window mounted flush with the interior surface at a position 2 cm upstream from the end plate. The shocks were

generated by high pressure hydrogen in a 1.7 m long driver section. The system was pumped off by an oil-diffusion pump to less than 1×10^{-4} Torr before each run. All experiments were performed behind reflected shock waves.

The concentration change of hydrogen bromide was monitored by $3.93 \mu\text{m}$ emission, which was detected by an AuGe detector at 77 K. The detector was coupled to an amplifier, whose output was displayed directly on an oscilloscope.

Hydrogen bromide was produced by dropping bromine on tetrahydronaphthalene.⁵⁾ The gas thus obtained was solidified and degassed at the temperature of liquid N_2 -ethanol slush and purified by trap to trap distillation at this temperature. Argon and nitrogen oxide from commercial cylinders were used without further purification.

The gas mixtures studied and the experimental conditions are listed in Table 1. Fig. 1 shows a typical oscillogram of

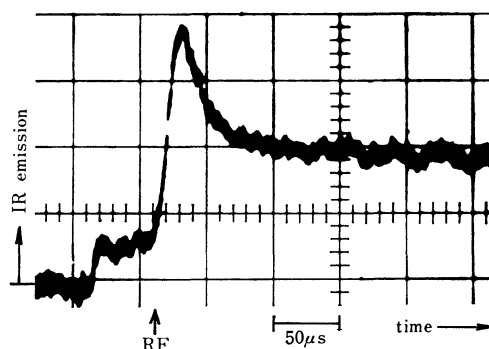


Fig. 1. Typical oscillogram of the experiments. Run No. 181; $T=2977 \text{ K}$, $\text{HBr}=5.955 \times 10^{-7} \text{ mol}/\text{cm}^3$, $\text{NO}=2.975 \times 10^{-7} \text{ mol}/\text{cm}^3$, $\text{Ar}=7.400 \times 10^{-6} \text{ mol}/\text{cm}^3$. The trace shows the IR emission at $3.93 \pm 0.1 \mu\text{m}$. RF indicates the time at which reflected shock front reached the window.

TABLE 1. SAMPLES AND EXPERIMENTAL CONDITIONS

	HBr (%)	NO (%)	Ar (%)	Total mol/cm ³	Pressure (atm)	Temperature (K)	Symbol
1)	8	8	84	$3.4\text{--}5.5 \times 10^{-6}$	0.7—0.95	2000—3030	○
2)	4	4	92	6.7—10	1.6—1.81	2180—2894	●
3a)	2	2	96	6.7—10.2	1.6—1.95	2244—3237	◐
3b)	2	2	96	17—22	3.4—3.8	2104—2485	◑
4)	2	4	94	7.1—11.3	1.9—2.2	2140—3000	◒
5)	8	4	88	7.4—13	1.8—2.2	2050—3350	◓
6)	2	7.1	90.9	7.7—12.6	1.8—2.2	2150—3150	●

the experiments. The slow rise of IR emission is due to the relatively long time constant of the AuGe detector. From the signals of two piezo-gauges, the shock speed was calculated.

Results and Discussion

The rate of HBr disappearance ($-d[\text{HBr}]/dt$) was obtained from the gradient of the IR emission intensity in an early stage of reaction. Figures 2, 3, and 4 show the Arrhenius plots of $-d[\text{HBr}]/dt$ for pairs of different samples. In Fig. 2, in each of these samples at about the same temperature the concentrations of NO and Ar are almost equal, but there are two- and four-fold differences in the concentration of HBr. In Fig. 3, there are differences in the concentration of NO, and in Fig. 4, the argon density is varied about two- and four-fold, holding the concentrations of the other reactants constant. The reaction orders with respect to the initial concentrations of HBr, NO, and Ar were obtained from these figures at 2500 K to be 1 ± 0.3 , 0.7 ± 0.2 , and 0 ± 0.1 , respectively. The fact that the reaction order with respect to Ar is small, nearly zero, implies that Reaction 2 becomes unimportant with the addition of NO. Later, we will find that this value of

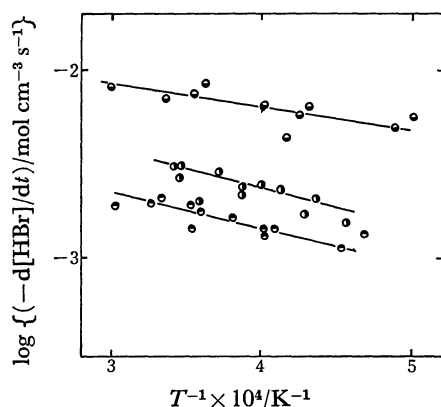


Fig. 2. Arrhenius plot of the rate of HBr disappearance for samples 2), 4), and 5). This figure shows that the reaction order for HBr is 1 ± 0.3 at 2500 K. Symbols are summarized in Table 1.

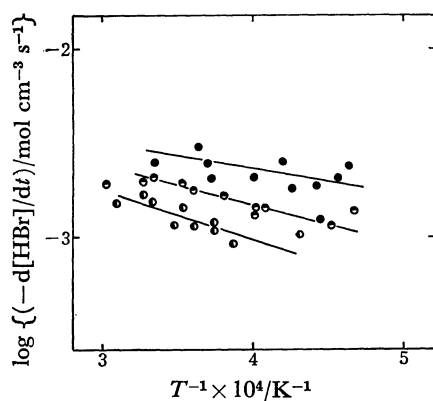


Fig. 3. Arrhenius plot of the rate of HBr disappearance for samples 3a), 4), and 6). This figure shows that the reaction order for NO is 0.7 ± 0.2 at 2500 K. Symbols are summarized in Table 1.

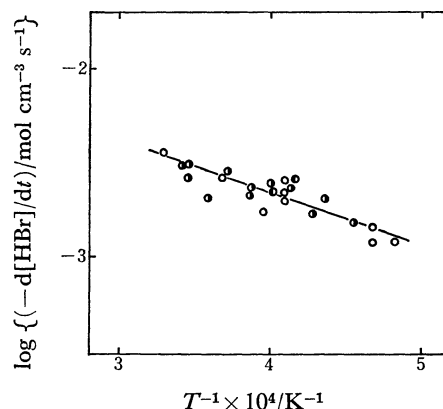


Fig. 4. Arrhenius plot of the rate of HBr disappearance for samples 1), 2), and 3b). This figure shows that the reaction order for Ar is 0 ± 0.1 at 2500 K. Symbols are summarized in Table 1.

the reaction order is in good agreement with the value ($0-0.1$) which was estimated from the calculations with an assumed reaction mechanism. From Fig. 3, the reaction order with respect to NO seems to decrease slightly with increasing temperature. This may be explained qualitatively by the fact that at higher temperatures Reaction 2 begins to contribute gradually to the rate of HBr disappearance (see Fig. 6). Thus, the overall rate equation can be expressed as

TABLE 2. ELEMENTARY REACTIONS AND KINETIC PARAMETERS, $k = AT^B \exp(-E/RT)$

Reaction	$\log A^a$	B	E (kcal/mol)	Ref.
1 $\text{HBr} + \text{NO} \rightarrow \text{HNO} + \text{Br}$	12.8	0.0	30.0	This work
2 $\text{HBr} + \text{Ar} \rightarrow \text{H} + \text{Br} + \text{Ar}$	12.19	0.0	50.0	4
3 $\text{HNO} + \text{Ar} \rightarrow \text{H} + \text{NO} + \text{Ar}$	16.5	0.0	49.0	6
4 $\text{HBr} + \text{H} \rightarrow \text{H}_2 + \text{Br}$	13.1	0.0	0.9	7
5 $\text{H}_2 + \text{Br} \rightarrow \text{HBr} + \text{H}$	14.43	0.0	19.7	8
6 $\text{HBr} + \text{Br} \rightarrow \text{H} + \text{Br}_2$	13.4	0.0	41.8	8
7 $\text{Br}_2 + \text{H} \rightarrow \text{HBr} + \text{Br}$	14.18	0.0	0.9	9
8 $\text{Br}_2 + \text{Ar} \rightarrow 2\text{Br} + \text{Ar}$	11.33	0.5	31.3	10
9 $\text{H}_2 + \text{Ar} \rightarrow 2\text{H} + \text{Ar}$	14.34	0.0	96.0	6
10 $\text{H} + \text{NO} \rightarrow \text{OH} + \text{N}$	13.7	0.0	48.7	1
11 $\text{N} + \text{NO} \rightarrow \text{N}_2 + \text{O}$	13.2	0.0	0.0	6
12 $\text{O} + \text{HBr} \rightarrow \text{OH} + \text{Br}$	12.38	0.0	2.7	11
13 $\text{OH} + \text{HBr} \rightarrow \text{H}_2\text{O} + \text{Br}$	12.5	0.0	0.0	12
14 $\text{H}_2\text{O} + \text{H} \rightarrow \text{H}_2 + \text{OH}$	13.97	0.0	20.6	6
15 $\text{OH} + \text{H} \rightarrow \text{H}_2 + \text{O}$	9.5	1.0	7.0	6
16 $2\text{H} + \text{Ar} \rightarrow \text{H}_2 + \text{Ar}$	17.81	-1.0	0.0	6
17 $2\text{Br} + \text{Ar} \rightarrow \text{Br}_2 + \text{Ar}$	12.9	0.0	-10.8	10
18 $\text{H}_2 + \text{O} \rightarrow \text{OH} + \text{H}$	10.25	1.0	9.96	6
19 $\text{H}_2 + \text{OH} \rightarrow \text{H}_2\text{O} + \text{H}$	13.35	0.0	5.2	6
20 $2\text{O} + \text{Ar} \rightarrow \text{O}_2 + \text{Ar}$	15.78	-0.5	0.0	6
21 $\text{O}_2 + \text{Ar} \rightarrow 2\text{O} + \text{Ar}$	14.41	0.0	108.0	6
22 $\text{H} + \text{O}_2 \rightarrow \text{OH} + \text{O}$	14.34	0.0	16.9	6
23 $\text{OH} + \text{O} \rightarrow \text{H} + \text{O}_2$	13.1	0.0	0.0	6
24 $\text{NO} + \text{O} \rightarrow \text{N} + \text{O}_2$	9.18	1.0	38.5	6
25 $\text{O} + \text{Br}_2 \rightarrow \text{BrO} + \text{Br}$	12.71	0.0	0.0	13
26 $\text{O} + \text{BrO} \rightarrow \text{O}_2 + \text{Br}$	13.61	0.0	0.0	14

a) Units: mol cm^{-3} for concentration, s for time.

$$-d[\text{HBr}]/dt = k_{\text{overall}}[\text{HBr}]^{1 \pm 0.3}[\text{NO}]^{0.7 \pm 0.2}[\text{Ar}]^{0 \pm 0.1}.$$

It is to be noted that this equation can be applied in an early stage of reaction. Reaction orders change with time, because Reactions 4–7, which are shown in Table 2, become predominant with time. Calculations of the reaction orders with time are discussed later and shown in Fig. 11. Figure 5 shows the Arrhenius plot of k_{overall} for all data obtained under various experimental conditions. It is found that all data points fall around one straight line. The best fit line gives the rate expression as

$$k_{\text{overall}} = 10^{10.4 \pm 0.2} \exp \{ -(23.2 \pm 3.0) \text{ kcal}/RT \} \text{ cm}^2 \cdot \text{l mol}^{-1} \text{ s}^{-1}.$$

To ascertain the influence of NO on the rate of HBr disappearance, a 4% HBr–96% Ar mixture was also shock-heated, and the second order rate constants, $k_{\text{second}} = (-d[\text{HBr}]/dt)/[\text{HBr}][\text{Ar}]$, were compared between the mixtures with and without NO (Fig. 6). In this figure, the data obtained by Giedt *et al.*⁴⁾ for HBr–Ar mixture are also shown by a broken line. In spite of the different experimental conditions and methods of data reduction in the two works, our rate data for HBr disappearance without NO are in good agreement with those of Giedt *et al.* It is also found, in Fig. 6, that the rate of HBr disappearance is accelerated by the addition of NO; this effect is remarkable at lower temperatures. Similar facts for HCl–NO–Ar mixtures³⁾ were also found in previous work.

To clarify the kinetics of HBr disappearance for mixtures involving NO, 26 elementary reactions (Mechanism I) were selected and tabulated in Table 2. Using tabulated rate constants for Reactions 2–26, concentration changes of HBr were calculated and were compared with the histories of HBr (IR intensity) obtained experimentally, where the emission intensity at zero time was determined by extrapolating the emission trace to the reflected shock front. In the calculations, since there are no rate data for Reaction 1, the value of k_1 was varied and then determined so as to fit the experimental histories of HBr at various temperatures. The value of k_1 thus determined is expressed as

$$k_1 = 10^{12.8} \exp (-30 \text{ kcal}/RT) \text{ cm}^3 \text{ mol}^{-1} \text{ s}^{-1}.$$

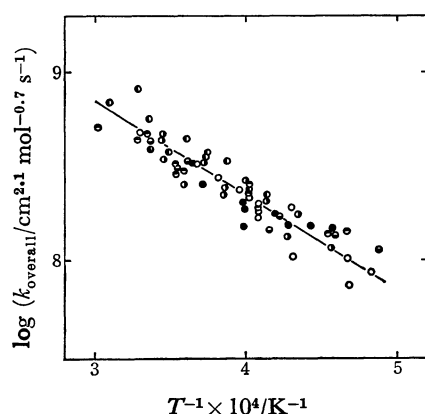


Fig. 5. Arrhenius plot of k_{overall} . Symbols are summarized in Table 1.

Examples of a fitting between the calculated and observed history are shown in Figs. 7a, b, c, and d for four cases under various experimental conditions. Figure 8 shows the time variations of the concentrations of HBr, NO, and the main products. As shown in this figure, NO does not decompose remarkably and the concentrations of N, O, OH, H₂O, and BrO are very low, at least in the early stages of reaction. Therefore, Mechanism I can be reduced to only the first eight elementary reactions (Mechanism II). The histories of HBr were also calculated by using Mechanism II and no discrepancy was found with those calculated with Mechanism I, implying that the rate of HBr disappearance was mainly governed by Reactions 1–8.

Sensitivity checks were performed on k_1 and k_2 for

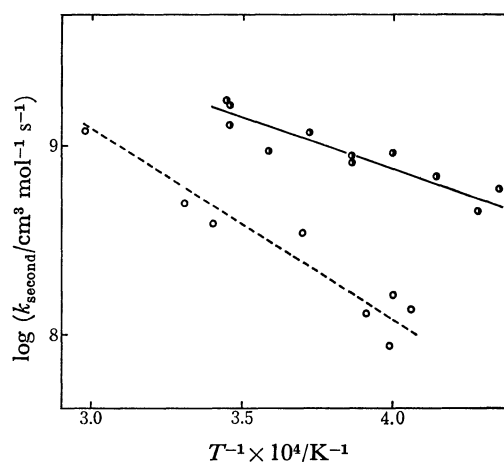


Fig. 6. Arrhenius plot of k_{second} for the mixtures with NO and without NO. ●: 4% HBr–4% NO–92% Ar, ○: 4% HBr–96% Ar, ---: calculated from the data of Giedt *et al.*⁴⁾.

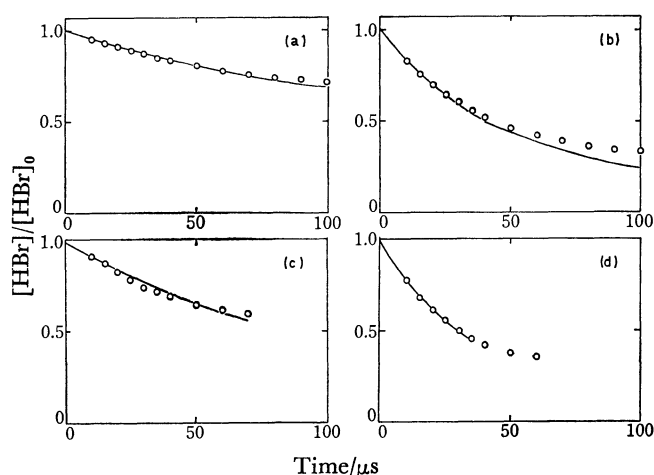


Fig. 7. Comparison of the histories of HBr obtained experimentally with those calculated. ○: Experiment, —: calculation. (a) Run No. 113; $T=2142$ K, $\text{HBr}=3.661 \times 10^{-7} \text{ mol/cm}^3$, $\text{NO}=3.661 \times 10^{-7} \text{ mol/cm}^3$, $\text{Ar}=4.576 \times 10^{-6} \text{ mol/cm}^3$. (b) Run No. 204; $T=2508$ K, $\text{HBr}=1.784 \times 10^{-7} \text{ mol/cm}^3$, $\text{NO}=6.337 \times 10^{-7} \text{ mol/cm}^3$, $\text{Ar}=8.925 \times 10^{-6} \text{ mol/cm}^3$. (c) Run No. 110; $T=2529$ K, $\text{HBr}=2.705 \times 10^{-7} \text{ mol/cm}^3$, $\text{NO}=2.075 \times 10^{-7} \text{ mol/cm}^3$, $\text{Ar}=3.381 \times 10^{-6} \text{ mol/cm}^3$. (d) Run No. 181; conditions are the same as Fig. 1.

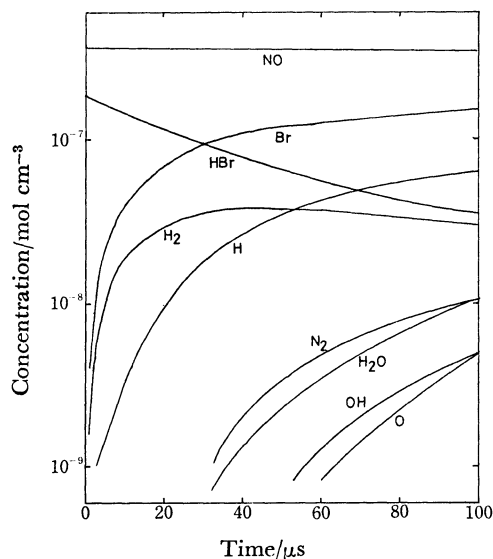


Fig. 8. Time dependent concentration changes of chemical species for Run No. 166. $T=2828$ K, $\text{HBr}=1.867 \times 10^{-7}$ mol/cm³, $\text{NO}=3.735 \times 10^{-7}$ mol/cm³, $\text{Ar}=9.337 \times 10^{-6}$ mol/cm³.

the purpose of examining how the overall rate of HBr disappearance was influenced by k_1 and k_2 . The values of k_1 and k_2 were varied in the ranges of 0 to 1.5 times and 0 to 2 times, respectively. The results of the calculations at temperatures 2179 and 2977 K are shown in Figs. 9 and 10, respectively. These figures show that the rate of HBr disappearance is remarkably influenced by the value of k_1 . On the other hand, at 2179 K the influence of the variation of k_2 is very little, while at 2977 K it becomes slightly appreciable. These facts suggest that Reaction 1 is more important than Reaction 2 for the rate of HBr disappearance at least in the low temperature region, and that the importance of Reaction 2 increases with increasing temperature.

Figure 11 shows the time variations of reaction orders with respect to the concentrations of HBr, NO, and Ar; these were calculated by using Mechanism I for the conditions of Run No. 110. When the reaction order for HBr was calculated, for example, the initial con-

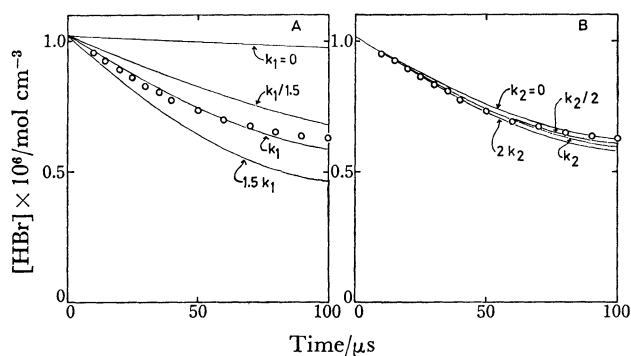


Fig. 9. Sensitivity of calculated HBr concentration to the value of k_1 (Fig. A) and k_2 (Fig. B) for Run No. 189. $T=2179$ K, $\text{HBr}=1.022 \times 10^{-6}$ mol/cm³, $\text{NO}=5.112 \times 10^{-7}$ mol/cm³, $\text{Ar}=1.278 \times 10^{-5}$ mol/cm³. \circ : Experimental history, —: histories calculated by using various values of k_1 and k_2 .

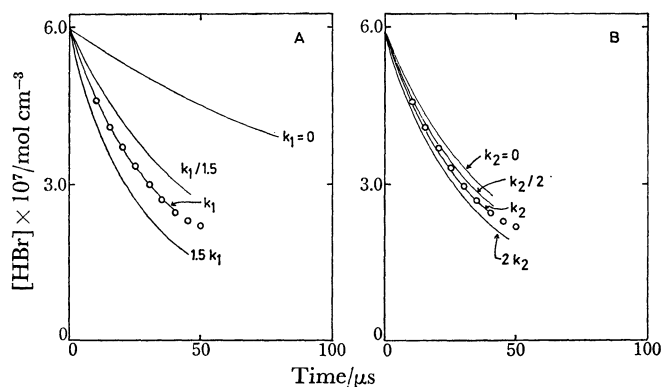


Fig. 10. Sensitivity of calculated HBr concentration to the values of k_1 (Fig. A) and k_2 (Fig. B) for Run No. 181. Conditions are the same as Fig. 1. \circ : Experimental history, —: histories calculated by using various values of k_1 and k_2 .

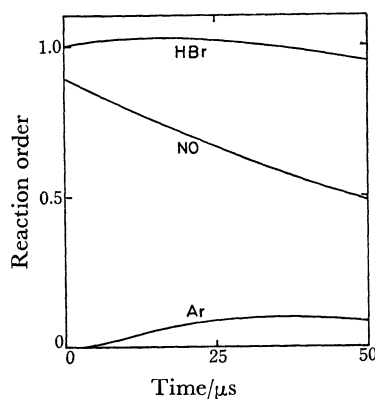


Fig. 11. Time variations of the reaction orders with respect to the initial concentrations of HBr, NO, and Ar for Run No. 110. Conditions are the same as Fig. 7 (c).

centration of HBr was changed by a factor of 2 and those of NO and Ar were not changed, then the rate of HBr disappearance was calculated and compared with that for the conditions of Run No. 110, where the rates were obtained as an average over every 2 μ s intervals, i.e., $-\text{d}[\text{HBr}]/\text{d}t = ([\text{HBr}]_t - [\text{HBr}]_{t-2})/2$. From Fig. 11, in the initial stage, the reaction orders are 1, 0.5–0.9, and 0–0.1 with respect to HBr, NO, and Ar, respectively. These calculated reaction orders are in good agreement with those determined experimentally, as mentioned already. Several calculated results showed that the reaction orders with respect to NO and Ar were dependent on the value of k_1 . That is, as the value of k_1 decreases, the reaction order for NO decreases and that for Ar increases. The agreement of the reaction orders between the calculation and the observation implies that the value of k_1 determined is reasonable.

The rate of HBr disappearance in Mechanism II is expressed as

$$-\text{d}[\text{HBr}]/\text{d}t = \underbrace{k_1[\text{HBr}][\text{NO}]}_{\text{term A}} + \underbrace{k_2[\text{HBr}][\text{Ar}]}_{\text{term B}} + \underbrace{k_4[\text{H}][\text{HBr}] - k_5[\text{H}_2][\text{Br}]}_{\text{term C}}$$

$$+ \underbrace{k_6[\text{HBr}][\text{Br}] - k_7[\text{Br}_2][\text{H}]}_{\text{term D}}.$$

The contributions of terms A, B, C, and D to the rate of HBr disappearance are shown in Fig. 12 as a function of time for the conditions of Run No. 110. This figure shows that terms A and C are dominant in the rate of HBr disappearance, confirming the importance of Reactions 1, 4, and 5.

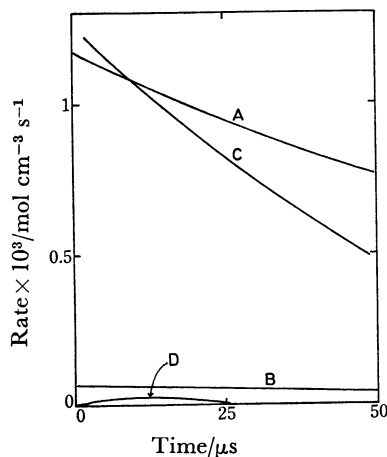


Fig. 12. Time variations of the rate terms which contribute to HBr disappearance for Run No. 110. Conditions are the same as Fig. 7(c). Terms A, B, C, and D are explained in the text.

Reaction B and Reaction 1 are expected to have similar activated complexes. According to the transition state theory, the ratio of k_B to k_1 is expressed as

$$k_B/k_1 = (F_{(\text{HBr})}/F_{(\text{HCl})}) \times (F_{(\text{HCl-NO})}^*/F_{(\text{HBr-NO})}^*) \times \exp \{-(E_{0(\text{B})} - E_{0(\text{I})})/RT\} \quad (\text{I})$$

where $F_{(\text{X})}$ is the partition function of species X, E_0 is the activation energy, and superscript \neq denotes activated complex. Assuming that the electronic and vibrational partition functions are canceled out, Eq. I can be rewritten as

$$\begin{aligned} k_B/k_1 &= (f_{\text{t}(\text{HBr})}/f_{\text{t}(\text{HCl})}) \times (f_{\text{r}(\text{HBr})}/f_{\text{r}(\text{HCl})}) \\ &\times (f_{\text{v}(\text{HCl-NO})}^*/f_{\text{v}(\text{HBr-NO})}^*) \times (f_{\text{r}(\text{HCl-NO})}^*/f_{\text{r}(\text{HBr-NO})}^*) \\ &\times \exp \{-(E_{0(\text{B})} - E_{0(\text{I})})/RT\} \\ &= (M_{(\text{HBr})}/M_{(\text{HCl})})^{3/2} \times (I_{(\text{HBr})}/I_{(\text{HCl})}) \\ &\times (M_{(\text{HCl-NO})}/M_{(\text{HBr-NO})})^{3/2} \\ &\times (I_{\text{A}(\text{HCl-NO})}I_{\text{B}(\text{HCl-NO})}I_{\text{C}(\text{HCl-NO})}/ \\ &\quad I_{\text{A}(\text{HBr-NO})}I_{\text{B}(\text{HBr-NO})}I_{\text{C}(\text{HBr-NO})})^{1/2} \\ &\times \exp \{-(E_{0(\text{B})} - E_{0(\text{I})})/RT\}, \quad (\text{II}) \end{aligned}$$

where f_{t} and f_{r} are the translational and rotational partition functions, respectively, M is the mass of the molecule or activated complex, and I is the moment of inertia. Activation energies and bond lengths of activated complexes were calculated by the BEBO method. In the calculations, the bond angles of the complexes were assumed to be 108.6° for O-N-H and 180° for N-H-X. Thus, from Eq. II we obtain

$$\begin{aligned} (k_B/k_1)_{\text{cal.}} &= (81/36.5)^{3/2} \times (3.30/2.71) \times (66.5/111)^{3/2} \\ &\times \{(1.72 \times 38.95 \times 40.67)/ \\ &\quad (1.82 \times 56.5 \times 58.36)\}^{1/2} \\ &\times \exp \{-(52.7 - 36.7) \text{ kcal}/RT\} \\ &= 1.26 \exp (-16.0 \text{ kcal}/RT). \quad (\text{III}) \end{aligned}$$

The ratio determined experimentally is

$$(k_B/k_1)_{\text{exp.}} = 2.51 \exp (-20.2 \text{ kcal}/RT). \quad (\text{IV})$$

The agreement between the calculated and experimental ratios seems very good.

References

- 1) H. Ando and T. Asaba, *Int. J. Chem. Kinet.*, **8**, 259 (1976).
- 2) M. Koshi, H. Ando, M. Oya, and T. Asaba, 15th Symp. (Int.) Combust., 1975, p. 809.
- 3) T. Higashihara, K. Saito, and I. Murakami, *Bull. Chem. Soc. Jpn.*, **51**, 3426 (1978).
- 4) R. R. Giedt, N. Choen, and T. A. Jacobs, *J. Chem. Phys.*, **50**, 5374 (1969).
- 5) *Inorg. Synth.*, **1**, 150 (1939).
- 6) D. L. Baulch, D. D. Drysdale, D. G. Home, and A. C. Lloyd, "Evaluated Kinetic Data for High Temperature Reactions," Butterworths, London (1972), Vol. 1; (1973), Vol. 2; D. L. Baulch, D. D. Drysdale, J. Duxbury, and S. Grant, *ibid.*, (1976), Vol. 3.
- 7) J. M. White, *J. Chem. Phys.*, **58**, 4482 (1973).
- 8) G. C. Fettes and J. H. Knox, *Prog. React. Kinet.*, **2**, 27 (1964).
- 9) B. A. Thrush, *Prog. React. Kinet.*, **3**, 88 (1965).
- 10) M. Warshaw, *J. Chem. Phys.*, **54**, 4060 (1971).
- 11) R. D. H. Brown and I. W. M. Smith, *Int. J. Chem. Kinet.*, **7**, 301 (1975).
- 12) G. A. Takacs and G. P. Glass, *J. Phys. Chem.*, **77**, 1060 (1972).
- 13) M. A. A. Clyne and H. W. Cruse, *Trans. Faraday Soc.*, **67**, 2869 (1971).
- 14) M. A. A. Clyne and H. W. Cruse, *Trans. Faraday Soc.*, **66**, 2227 (1970).